Enhanced Higgs boson coupling to charm pairs

Cédric Delaunay,[1,2] Tobias Golling,[3] Gilad Perez,[2,4] and Yotam Soreq[4]

[1]*LAPTh, Université de Savoie, CNRS, B.P. 110, F-74941 Annecy-le-Vieux, France*
[2]*CERN, Theory Division, CH-1211 Geneva 23, Switzerland*
[3]*Department of Physics, Yale University, New Haven, Connecticut 06520, USA*
[4]*Department of Particle Physics and Astrophysics, Weizmann Institute of Science, Rehovot 76100, Israel*

We show that current Higgs data permit a significantly enhanced Higgs coupling to charm pairs, comparable to the Higgs-to-bottom pairs coupling in the Standard Model, without resorting to additional new physics sources in Higgs production. With a mild level of the latter current data even allow for the Higgs-to-charm pairs to be the dominant decay channel. An immediate consequence of such a large charm coupling is a significant reduction of the Higgs signal strengths into the known final states as in particular into bottom pairs. This might reduce the visible vector-boson associated Higgs production rate to a level that could compromise the prospects of ever observing it. We however demonstrate that a significant fraction of this reduced signal can be recovered by jet-flavor tagging targeted towards charm-flavored jets. Finally we argue that an enhanced Higgs-to-charm pairs coupling can be obtained in various new physics scenarios in the presence of only a mild accidental cancellation between various contributions.

I. INTRODUCTION

The recent discovery of a Higgs-like particle at the LHC [1,2] is a remarkable success of the Standard Model (SM) of particle physics. The current data imply that the new particle is consistent with the SM predictions [3,4]. Still, a lot is yet to be learned regarding the properties of this recently discovered particle.

It is important to study the nature of the Higgs couplings to other SM fields. As the Higgs is rather light, with a mass smaller than that of the top quark and smaller than twice the mass of the W and Z bosons, it decays to particles that very weakly interact with it. In fact, the dominant decay mode of the Higgs is to a bottom pair within the SM, and the bottom Yukawa coupling to an on-shell Higgs is $\mathcal{O}(0.02)$. This exposes the Higgs branching ratios to a generic susceptibility to any form of new physics. Any deformation of the Higgs couplings to the SM particles or introduction of additional couplings to new fields that competes with the small Higgs-to-bottom coupling will lead to a significant change of the Higgs phenomenology at the LHC. An interesting picture emerges from the potential changes to the existing Higgs couplings to SM particles. The next-to-leading five couplings beyond the bottom coupling are Higgs couplings to W, Z and τ, which are already measured to decent accuracy, the coupling to gluons which controls the Higgs production cross section, and the coupling to the charm quark. Among those SM states the charm stands out as almost nothing is known experimentally on its coupling to the Higgs boson.

The Higgs branching ratio into charm pairs is $\mathcal{O}(3\%)$ in the SM, which renders any attempt to directly probe the Higgs-to-charm coupling at the LHC extremely challenging due to the large multijet background. However, the charm Yukawa coupling is only a few times smaller than the bottom one in the SM, about one part in five at the Higgs mass scale [5]. Thus, only a factor of a few mismatch between the actual charm coupling and its SM value would lead to a significant change of the Higgs phenomenology. Furthermore, despite its small value, the charm mass is not negligible and due to the Cabibbo-Kobayashi-Maskawa (CKM) suppression in bottom decays the charm lifetime is comparable to that of the bottom quark. Hence, jets originating from charm quarks can in principle be identified at colliders. The ATLAS Collaboration, in fact, recently presented new experimental techniques designed to tag charm jets at the LHC [6]. The possibility to apply charm tagging, beyond its plain interest from the SM perspective [7,8], also opens new possibilities to analyze various beyond the SM signals [9–12]. In particular we show in this paper how crucial charm tagging may be in order to exhume the associated Higgs production signal in the case of a suppressed $h \to b\bar{b}$ branching ratio due to an enhanced Higgs-to-charm coupling relative to the SM.

There is currently no attempt to directly probe the $h \to c\bar{c}$ channel at colliders and the Higgs-to-charm coupling is constrained indirectly through the bound on the allowed Higgs "invisible" (more precisely, unobserved) branching ratio. For SM Higgs production cross sections this branching ratio cannot exceed $\sim 20\%$ at 95% confidence level (C.L.), or $\sim 50\%$ if an additional new physics source of gluon fusion production is assumed [3]. This implies a rough upper bound on the Higgs-to-charm coupling of

about 3 to 5 times its SM value, assuming no other source of invisible decays other than Higgs decays into the unobserved SM states.[1] Hence, the current data still allow for the $h \to c\bar{c}$ decay channel to be comparable in size with or even to dominate over the $h \to b\bar{b}$ one.

The outline of the paper is as follows. In the next section we provide a quantitative analysis of the current Higgs data in order to derive the present bounds on the Higgs-to-charm coupling. We then demonstrate in Sec. III that an enhanced charm coupling significantly suppresses the $h \to b\bar{b}$ signal strength in associated Higgs production, mostly through a reduced Higgs branching ratio into bottom pairs, and that the SM level of this signal could be partially or even entirely recovered by enriching the sample with charm-tagged events, depending on the charm-tagging efficiency. In Sec. IV, we argue that a large Higgs-to-charm coupling can be obtained under reasonable conditions in various theories beyond the SM where moderate cancellation is present. We present our conclusions in Sec. V.

II. CONSTRAINTS FROM HIGGS DATA

A Higgs-to-charm pair coupling significantly larger than in the SM affects both Higgs production cross sections and branching ratios, and is therefore indirectly constrained by current Higgs rate measurements at the LHC. On the one hand a large Higgs-to-charm coupling implies a universal reduction of all Higgs branching ratios other than into $c\bar{c}$ final states, provided all other Higgs couplings remain standard. On the other hand Higgs production at hadron colliders is also typically enhanced relative to the SM through a more important charm fusion mechanism occurring at tree level. (Another effect, though far subdominant, arises in gluon fusion Higgs production through a modified charm-loop contribution.) Therefore, one might expect that there is a charm coupling value for which the enhancement in Higgs production approximately compensates the universal suppression in Higgs decays so that Higgs rates measured at the LHC remain close to the SM predictions. We thus perform a fit of all available Higgs data allowing deviations of the $hc\bar{c}$ coupling relative to the SM in order to quantitatively determine the largest value presently allowed.

We follow the approach of Ref. [3] to globally fit available Higgs data. We consider both direct data from Higgs rate measurements at the LHC and indirect constraints from electroweak (EW) precision measurements at the LEP. We assume that there is only one Higgs scalar h of mass $m_h = 126$ GeV, which is a singlet of the custodial symmetry preserved by EW symmetry breaking (EWSB). The Higgs interactions with other SM particles are assumed to be flavor conserving and accurately enough parametrized by the effective Lagrangian

$$\mathcal{L}_{\text{eff}} = \mathcal{L}_0 + \mathcal{L}_2, \tag{1}$$

where interactions to zeroth order in derivatives are

$$\mathcal{L}_0 = \frac{h}{v}\left[c_V(2m_W^2 W_\mu^+ W^{\mu-} + m_Z^2 Z_\mu Z^\mu) \right.$$
$$\left. - \sum_q c_q m_q \bar{q}q - \sum_\ell c_\ell m_\ell \bar{\ell}\ell \right], \tag{2}$$

and interactions to next-to-leading order in derivatives are

$$\mathcal{L}_2 = \frac{h}{4v}[c_{gg}G_{\mu\nu}^a G^{\mu\nu a} - c_{\gamma\gamma}F_{\mu\nu}F^{\mu\nu} - 2c_{WW}W_{\mu\nu}^+ W^{\mu\nu-}$$
$$- 2c_{Z\gamma}F_{\mu\nu}Z^{\mu\nu} - c_{ZZ}Z_{\mu\nu}Z^{\mu\nu}], \tag{3}$$

where $q = u, d, s, c, b, t$ and $\ell = e, \mu, \tau$ are the SM massive quarks and charged leptons, $v = 246$ GeV is the EWSB scale, and W_μ, Z_μ, A_μ and G_μ are the SM gauge fields with the corresponding fields strength tensors. The tree-level SM limit is achieved by $c_V = c_q = c_\ell = 1$ and $c_{\gamma\gamma} = c_{gg} = c_{Z\gamma} = 0$ (before the top quark has been integrated out). We neglect operators which are odd under the product of charge conjugation and parity transformations (CP) and assume real $c_{q,\ell}$ coefficients as there is only a weak sensitivity to CP-odd couplings and CP-violating phases in Higgs rate measurements.[2] (See e.g. Ref. [16] for a recent update.) The underlying custodial symmetry imposes the following relations among couplings in $\mathcal{L}_2$ [3]:

$$c_{WW} = c_{\gamma\gamma} + \frac{g_L}{g_Y}c_{Z\gamma}, \qquad c_{ZZ} = c_{\gamma\gamma} + \frac{g_L^2 - g_Y^2}{g_Y g_L}c_{Z\gamma}, \tag{4}$$

where g_L and g_Y are the SU(2)$_L$ and U(1)$_Y$ gauge couplings, respectively. In contrast with existing Higgs fits, as in e.g. Refs. [3,4,17,18], we leave the c_c as a free parameter of the fit. Current Higgs data are very unlikely to be sensitive to Higgs couplings to e, μ, and u, d, s, as the latter are already very small in the SM. We thus set $c_{e,\mu} = c_{u,d,s} = 1$ in the following. We are left with at most eight independent free parameters: c_V, $c_{c,b,t}$, c_τ, c_{gg}, $c_{\gamma\gamma}$ and $c_{Z\gamma}$.

The Higgs rate measurements at the LHC are presented in the form of signal strengths defined as

$$\mu_f \equiv \frac{\sigma_{pp\to h}\text{BR}_{h\to f}}{\sigma_{pp\to h}^{\text{SM}}\text{BR}_{h\to f}^{\text{SM}}}, \tag{5}$$

for each final state f, where $\sigma_{pp\to h}$ and $\text{BR}_{h\to f}$ are the Higgs production cross section and branching ratio, respectively, while the $^{\text{SM}}$ label denotes their corresponding SM predictions. Similar signal strengths measured at the Tevatron are obtained from Eq. (5) through the replacement

---

[1]The observation that a sizable enhancement of the Higgs-to-charm coupling relative to the SM is still allowed by current Higgs data was also pointed out in Ref. [13].

[2]Higher sensitivities to CP-odd couplings may be reached for instance through angular distribution measurements, in particular in vector-boson associated Higgs production channels where the Higgs boson can be significantly boosted [14,15].

$pp \rightarrow p\bar{p}$. We perform a standard χ^2 analysis in order to fit the coefficients in Eq. (1) to current Higgs data. The total χ^2 function is

$$\chi^2 = \sum_{f,i} \frac{(\mu_{f,i}^{\text{th}} - \mu_{f,i}^{\text{ex}})^2}{\sigma_{f,i}^2}, \qquad (6)$$

where the index i runs over all measurements of the channel f and correlations between different channels are neglected. $\mu_{f,i}^{\text{ex}}$ and $\sigma_{f,i}$ denote the experimental central values and their corresponding standard deviations, respectively. Asymmetric experimental errors are symmetrized for simplicity. We consider the most updated set of Higgs measurements in $h \rightarrow WW^*$, ZZ^* and $\gamma\gamma$ channels from the ATLAS [19], CMS [20] and Tevatron [21] collaborations, as well as the $h \rightarrow \tau\tau$ results from CMS [22] and Tevatron [21]. We also include the recent $h \rightarrow b\bar{b}$ search in vector-boson associated production [23] and in vector-boson fusion at CMS [24], as well as the $h \rightarrow Z\gamma$ search at CMS [25]. We do not use the recent $h \rightarrow b\bar{b}$ and $h \rightarrow \tau\tau$ preliminary ATLAS results. However, we checked that the latter does not significantly change our results given the current experimental sensitivity in these channels. $\mu_{f,i}^{\text{th}}$ are the theoretical signal strength predictions, which incorporate the relative weights of each Higgs production mechanisms as quoted by the experimental collaborations, whenever available. This is the case for all channels that we use except for $Vh(b\bar{b})$ at CMS for which we assume pure vector-boson associated production. Theoretical predictions for Higgs signal strengths in terms of the effective coefficients in Eq. (1) can be found in Ref. [3], while we use the SM Higgs production cross sections and branching ratios of Ref. [26]. We however add the following two modifications in order to implement a $hc\bar{c}$ coupling significantly different than its SM value. First of all, we include the charm-loop contribution in the gluon fusion cross section as $\sigma_{gg\rightarrow h}/\sigma_{gg\rightarrow h}^{\text{SM}} \simeq |\hat{c}_{gg}|^2/|\hat{c}_{gg}^{\text{SM}}|^2$ with

$$\hat{c}_{gg} = c_{gg} + [1.3 \times 10^{-2} c_t - (4.0 - 4.3i) \times 10^{-4} c_b$$
$$- (4.4 - 3.0i) \times 10^{-5} c_c], \qquad (7)$$

where numbers are obtained using the running quark masses extracted from Ref. [5]. $\hat{c}_{gg}^{\text{SM}} \simeq 0.012$ is obtained by taking the SM limit, $c_{gg} \rightarrow 0$ and $c_{t,b,c} \rightarrow 1$, in Eq. (7). Then, we include the charm fusion cross section as $\sigma_{c\bar{c}\rightarrow h} \simeq 3.0 \times 10^{-3} |c_c|^2 \sigma_{gg\rightarrow h}^{\text{SM}}$, where the charm fusion to gluon fusion cross section ratio is evaluated at next-to-leading order in the QCD coupling and we use MSTW parton distribution functions [27]. We transposed the next-to-leading order bottom fusion cross section obtained in Ref. [28] in order to estimate $\sigma_{c\bar{c}\rightarrow h}^{\text{SM}}$.

We mainly focus on two different scenarios, where

(a) all Higgs couplings but the charm one are SM-like;

(b) all the Higgs couplings but the charm one and c_{gg} are SM-like.

The general case, where all independent parameters are allowed to deviate from the SM is discussed in Appendix A. However, the results are found to be very close to those from case (b) above. Thus, unless explicitly mentioned otherwise, case (b) can be taken as a proxy for the general case. In both cases (a) and (b), χ^2 only depends on the Higgs-to-charm coupling through $|c_c|^2$, up to a small interference effect with top and bottom loops in gluon fusion production. Hence, there is almost no sensitivity to the sign of c_c. For simplicity we consider positive c_c in the following. χ^2 minimization yields

$$c_c \leq 3.7(7.3), \quad \text{at } 95.4\% \text{ C.L.}, \qquad (8)$$

for case (a) [case (b)] as defined above. The bound in case (b) is obtained upon marginalizing over the c_{gg} coupling. The larger allowed range for the charm coupling in case (b) relative to case (a) is due to a further enhancement of the Higgs production cross section from $c_{gg} > 0$. $\delta\chi^2 \equiv \chi^2 - \chi_{\min}^2$ as a function of c_c for both cases is shown in Fig. 1. The $\delta\chi^2$ raise in case (b) for $c_c \gtrsim 3$ is due to the further universal suppression in the branching ratios induced by the larger $c_{gg} > 0$ values required to compensate for the increase in c_c. For case (b), we also show in Fig. 2 the 68.3% and 95.4% C.L. regions in the $c_c - c_{gg}$ plane. $h \rightarrow WW^*$ is the most significant channel which dominantly drives the χ^2 fit. Since $\mu_{WW^*} \lesssim 1$ at both ATLAS and CMS experiments, a total Higgs width slightly larger than in the SM is favored. This results in the fact that the χ^2 takes a minimum at a larger charm coupling, $c_c \gtrsim 1$, as shown in Fig. 1. Excluding the $h \rightarrow WW^*$ channel, the remaining average signal strength becomes $\gtrsim 1$ and the χ^2 fit favors lower values of c_c.

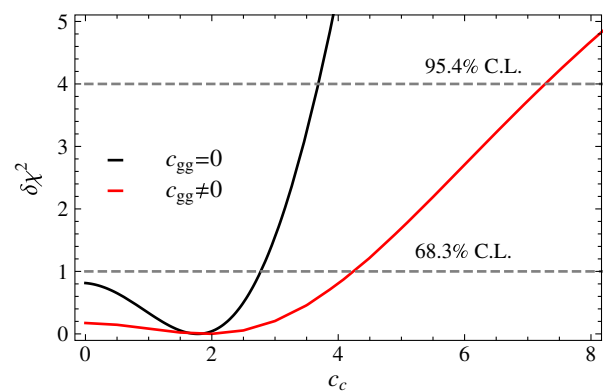We conclude that without additional new physics contributions to Higgs production other than the contribution

FIG. 1 (color online). $\delta\chi^2 = \chi^2 - \chi_{\min}^2$ as a function of the Higgs-to-charm pairs coupling c_c. The black and red curves correspond, respectively, to case (a), where all Higgs couplings but c_c are SM-like, and case (b), where only c_c and c_{gg} deviate from the SM and marginalizing over the latter. Horizontal dashed lines denote the 68.3% and 95.4% C.L. ($\delta\chi^2 = 1$ and 4, respectively).
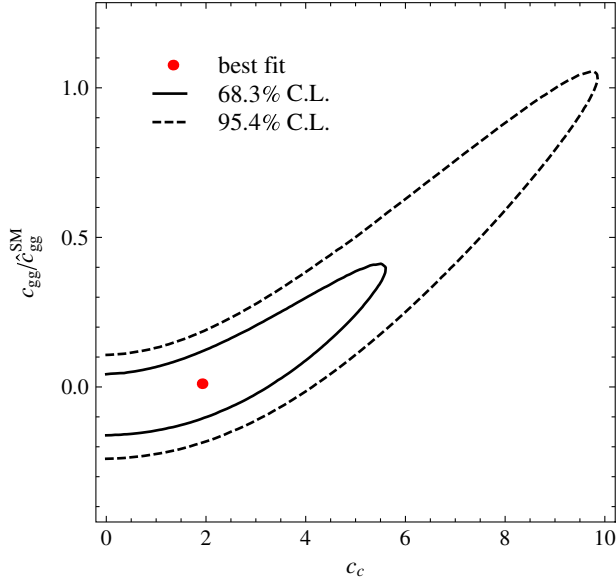
FIG. 2 (color online). The 68.3% (solid) and 95.4% (dashed) C.L. regions in the $c_c - c_{gg}$ plane in case (b) where only the Higgs-to-charm and Higgs-to-gluon couplings are allowed to deviate from their SM values. The red dot represents the best fit point. $\hat{c}_{gg}^{SM} \simeq 0.012$.

to charm and gluon fusion, the latter being subdominant, a Higgs-to-charm coupling as large as about 4 times its SM value is consistent with current Higgs data within 95.4% C.L. Even larger charm couplings are allowed at 95.4% C.L., provided that there is a conjoint $\mathcal{O}(1)$ enhancement in gluon fusion production from a new physics source. Such a large $hc\bar{c}$ coupling would in particular significantly reduce the Higgs branching ratio in bottom pairs. Consequently, suppressed $h \to b\bar{b}$ signals in vector-boson associated Higgs production at the ATLAS and CMS experiments are expected as these channels are much less sensitive to gluon fusion and $c\bar{c}$ fusion production mechanisms. Needless to say even bigger effects are found when the other couplings are allowed to float as well, in particular the Higgs-to-gluons effective coupling.

III. OBSERVABILITY OF $h \to c\bar{c}$ AT THE LHC

We showed in the previous section that a Higgs coupling to $c\bar{c}$ significantly larger than in the SM is allowed by current Higgs data. We argue here that such a large coupling yields important effects in channels where the Higgs boson decays into bottom pairs. In particular, one expects a significant suppression of $\mu_{b\bar{b}}$ in vector-boson associated production, due to a sizable enhancement of $BR_{h\to c\bar{c}}$ relative to the SM. We also demonstrate that the associated production signal can be partially recovered by using the recently developed charm-tagging technique [6].

We identify the following three interesting phenomenological aspects of having a large Higgs-to-charm coupling. First of all, $b\bar{b}$ signal strengths in associated production are

suppressed due to the larger Higgs width which reduces the branching ratio into bottom pairs as[3]

$$\frac{BR_{h\to b\bar{b}}}{BR_{h\to b\bar{b}}^{SM}} = \left[1 + (|c_c|^2 - 1)BR_{h\to c\bar{c}}^{SM} \right. \\ \left. + \left(\left|\frac{c_{gg}}{\hat{c}_{gg}^{SM}} + 1\right|^2 - 1\right)BR_{h\to gg}^{SM}\right]^{-1}. \quad (9)$$

Equations (8) and (9) show that enhancing the $hc\bar{c}$ coupling results in a significant reduction in the Higgs-to-bottom pairs rate in associated production processes $Vh(\bar{b}b)$ of

$$\mu_{b\bar{b}} \simeq 0.74(0.40), \quad (10)$$

for case (a) [(b)], respectively, where we assumed SM-like Vh production and no acceptance for the other production mechanisms. The suppressed signal in Eq. (10) is still consistent at 95.4% C.L. with all other existing Higgs data. This result makes this final state extremely challenging for the next run of the LHC. Note that in case (b) we include the subdominant Higgs width increase coming from $c_{gg} > 0$, which further suppresses $BR_{h\to b\bar{b}}$.

Second, we stress that there is a correlation between the measured $\mu_{b\bar{b}}$ and $\mu_{c\bar{c}}$ signal strengths, as the production cross section is identical for both channels and increasing the Higgs-to-charm coupling ($c_c > 1$) leads to a suppressed branching ratio into $b\bar{b}$ and an enhanced one into $c\bar{c}$. More precisely the signal strengths into bottom and charm pairs are simply proportional to each other, $\mu_{c\bar{c}} = |c_c/c_b|^2\mu_{b\bar{b}}$. Deviations of the bottom coupling from the SM limit are much more constrained by Higgs data than for the charm coupling [see Eq. (A1)], which yields $\mu_{c\bar{c}} \simeq |c_c|^2\mu_{b\bar{b}}$. Moreover, we find that this strong correlation remains also in the presence of an additional new physics source of gluon fusion production ($c_{gg} \neq 0$), as illustrated in Fig. 3 which shows the regions of the $\mu_{b\bar{b}} - \mu_{c\bar{c}}$ plane consistent within 68.3% and 95.4% C.L. with Higgs data. The signal strengths in Fig. 3 are evaluated assuming the relative weights of Higgs production mechanisms used by the CMS $b\bar{b}$ search in associated Higgs production [23]. Figure 3 also shows that in the case that c_c, c_{gg} and c_b are all allowed to vary, the above correlation still endures, albeit in a weaker way.

Finally, we find that the expected combined signal strength into bottom and charm pairs can be relatively enhanced compared to that of only bottom pairs, despite the smaller charm-tagging efficiency. We define the combined signal strength into $b\bar{b}$ and $c\bar{c}$ as

$$\mu_{b\bar{b}+c\bar{c}} \equiv \frac{\sigma_{pp\to h}(\varepsilon_b^2 BR_{h\to b\bar{b}} + \varepsilon_c^2 BR_{h\to c\bar{c}})}{\sigma_{pp\to h}^{SM}(\varepsilon_b^2 BR_{h\to b\bar{b}}^{SM} + \varepsilon_c^2 BR_{h\to c\bar{c}}^{SM})}, \quad (11)$$

---

[3]We neglected in Eq. (9) the subdominant effect of the Higgs-to-charm coupling in the loop-induced $h \to gg$ partial width.
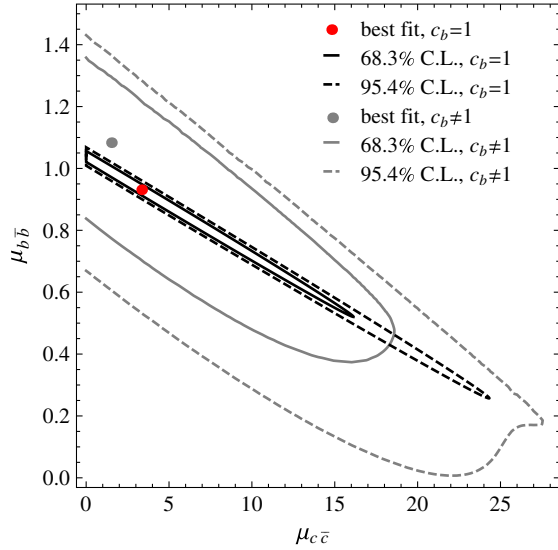
FIG. 3 (color online). Correlation between $\mu_{c\bar{c}}$ and $\mu_{b\bar{b}}$ signal strengths in the presence of an enhanced Higgs-to-charm coupling relative the SM. Relative weights of each of the Higgs production mechanisms from the CMS analysis [23] are assumed for both signal strengths. The red dot represents the best fit point and the solid (dashed) black line is the 68.3% (95.4%) C.L. contour derived from fitting current Higgs data for case (b), where only c_c and c_{gg} are not SM-like. The solid (dashed) gray contour delineates the allowed 68.3% (95.4%) C.L. region for the more general case where c_b is allowed to vary as well.

where ε_b and ε_c are the tagging efficiencies for bottom and charm jets, respectively. We implicitly assumed in Eq. (11) that the only difference between $c\bar{c}$ and $b\bar{b}$ analyses is the tagging efficiency, and that, in particular, the production cross section is the same in both cases. We also define the ratio of the combined and bottom-only signal strengths as

$$R \equiv \frac{\mu_{b\bar{b}+c\bar{c}}}{\mu_{b\bar{b}}} = \frac{1 + |c_c|^2 r_{cb}^2 \mathrm{BR}^{\mathrm{SM}}_{h \to c\bar{c}}/\mathrm{BR}^{\mathrm{SM}}_{h \to b\bar{b}}}{1 + r_{cb}^2 \mathrm{BR}^{\mathrm{SM}}_{h \to c\bar{c}}/\mathrm{BR}^{\mathrm{SM}}_{h \to b\bar{b}}}, \quad (12)$$

where $r_{cb} \equiv \varepsilon_c/\varepsilon_b$ is the ratio of tagging efficiencies of charm- and bottom-flavored jets. Assuming the branching ratio values for a 126 GeV SM Higgs [26], the upper bound from Eq. (8) derived from fitting current Higgs data implies

$$R \lesssim 1 + 0.21(0.86) \times \left(\frac{r_{cb}}{0.57}\right)^2, \quad (13)$$

for the case (a) [(b)] defined above, where $r_{cb} \simeq 0.57$ corresponds to $\varepsilon_b \simeq 0.7$ [23] together with a prospective charm-tagging efficiency of $\varepsilon_c \simeq 0.4$. The parameter R only measures how much combining charm and bottom pairs enhances the associated production signal relative to a sample of bottom pairs only. In particular it is independent of the production cross section by construction. The enhancement in Eq. (13) is to be compared with the much

reduced signal strength available when only b tagging is used to extract the signal, as given in Eq. (10). Combining Eqs. (10) and (13) yields a combined signal strength of

$$\mu_{b\bar{b}+c\bar{c}} = 0.89(0.75), \quad (14)$$

for case (a) [(b)], where $\varepsilon_c \simeq 0.4$ as well as pure SM-like vector-boson associated production are assumed.

We showed that the expected bottom pair signal strength in associated Higgs production can be significantly reduced, relative to the SM, in the presence of a largely enhanced $hc\bar{c}$ coupling, since the Higgs decay to charm pairs is becoming as important. Moreover, Eq. (13) shows that an increased tagging efficiency for charm jets can bring the measured associated Higgs production signal strength almost back to its SM level.

IV. CHARM COUPLING BEYOND THE SM

Modified Higgs couplings to fermions can arise in many theories beyond the SM. We consider here different theoretical frameworks which illustrate the possibility of having a Higgs-to-charm coupling significantly larger than within the SM. We begin with an effective field theory (EFT) discussion, where new physics above the weak scale is described by a set of higher-dimensional operators, in order to stress that Higgs coupling to charm is *a priori* not necessarily related to the small charm mass. We then discuss how much the Higgs-to-charm coupling can deviate from the SM within specific new physics scenarios. In particular, we show that it is possible to obtain c_c of order of a few, with all other couplings SM-like, in a two Higgs doublet model (2HDM) with minimal flavor violation (MFV) and in a general MFV (GMFV) [29] scenario with only one Higgs doublet. We finally comment on composite models where the Higgs field is realized as a pseudo-Nambu–Goldstone boson (pNGB).

Within the EFT framework the Higgs-to-charm coupling is modified in the presence of a dimension-six operator. The relevant operators in the up-type quark sector are

$$\mathcal{L}_{\mathrm{EFT}} \supset \lambda^u_{ij}\bar{Q}_i \tilde{H} U_j + \frac{g^u_{ij}}{\Lambda^2}\bar{Q}_i \tilde{H} U_j (H^\dagger H) + \mathrm{H.c.}, \quad (15)$$

where the first term is the marginal up-type Yukawa operator of the SM and the second term is a dimension-six operator suppressed by the new physics scale Λ. Q_i and U_i, with $i = 1, 2, 3$, are the SM quark left-handed doublets and right-handed singlets, respectively, and H is the Higgs doublet, with $\tilde{H} = i\sigma_2 H^*$. λ^u and g^u are generic complex 3×3 matrices in flavor space. Setting the Higgs field to its vacuum expectation value $H = (0, (v + h)/\sqrt{2})^T$, the mass and linear Higgs coupling matrices are, respectively,

$$M^u_{ij} = \frac{v}{\sqrt{2}}\left(\lambda^u_{ij} + g^u_{ij}\frac{v^2}{2\Lambda^2}\right), \quad (16)$$

$$Y_{ij}^u = \frac{1}{\sqrt{2}}\left(\lambda_{ij}^u + 3g_{ij}^u \frac{v^2}{2\Lambda^2}\right). \tag{17}$$

We assume for convenience that λ^u and g^u are aligned and that only $g_{22}^u \neq 0$ in the mass basis. In this case the deviation from the SM Higgs-to-charm coupling is simply

$$c_c = 1 + \frac{3}{2}\frac{v^2}{\Lambda^2}\frac{g_{22}^u}{y_c}, \tag{18}$$

where we defined $y_c \equiv \sqrt{2}m_c/v \simeq 3.6 \times 10^{-3}$, m_c being the running charm quark at the Higgs mass scale [5]. Naive dimensional analysis suggests that the effective description breaks down at the scale Λ for $g_{22}^u \sim 16\pi^2$. As a function of the Higgs-to-charm coupling modification this scale is

$$\Lambda \simeq \frac{63 \text{ TeV}}{\sqrt{|c_c - 1|}}. \tag{19}$$

Assuming the upper bound on c_c in Eq. (8), we find that the cutoff scale can be as high as $\Lambda \lesssim 38(25)$ TeV for case (a) [(b)]. These scales are sufficiently high so that it is possible that the associated new physics dynamics at the cutoff leaves no direct signatures at the LHC other than a significantly enhanced Higgs-to-charm coupling.

We now focus on some specific new physics scenarios. Consider a 2HDM with MFV [30,31]. In this setup, the MFV ansatz allows us to write the SM-like Higgs couplings to fermions as an expansion in the spurionic parameters which break the flavor symmetry group. Following notations of Ref. [32], the charm and top quark couplings to the SM-like Higgs boson are

$$c_t \simeq A_S^U + B_S^U y_t^2 + C_S^U y_b^2 |V_{tb}|^2,$$
$$c_c \simeq A_S^U + B_S^U y_c^2 + C_S^U (y_b^2 |V_{cb}|^2 + y_s^2 |V_{cs}|^2), \tag{20}$$

where $y_i \equiv \sqrt{2}m_i/v$, V_{ij} are the CKM matrix elements and A_S^U, B_S^U and C_S^U are $\mathcal{O}(1)$ coefficients. $\mathcal{O}(y_i^4)$ and higher contributions were neglected in Eq. (20). Assuming for instance $A_S^U \simeq 4$ and $B_S^U \simeq -3$, Eq. (20) yields $c_c \simeq 4$ and $c_t \simeq 1$. Moreover, in the limit where all the heavier Higgs states are decoupled, $c_V \simeq 1$ [33]. Therefore, a significantly larger charm coupling, with all other couplings close to their SM values, can be obtained at the expense of a mild cancellation, at the level of one part in a few, among unknown $\mathcal{O}(1)$ coefficients.

Consider now a model with one Higgs doublet in the GMFV framework [29], in which large top Yukawa effects are resummed to all orders. We define our notations in Appendix B. In the mass basis, the up-type quark mass and linear Higgs interaction matrices become $M^u \simeq \lambda v/\sqrt{2} \times$ diag$(y_u(\gamma + \zeta x), y_c(\gamma + \zeta x), 1 + rx)$ and to leading order in $\lambda_C \simeq 0.23$, the sine of the Cabibbo angle and in $x \equiv v^2/(2\Lambda^2)$, with Λ the GMFV scale, we find

$$Y^u \simeq \frac{\lambda}{\sqrt{2}}\begin{pmatrix} y_u(\gamma + 3\zeta x) & 0 & 2\lambda_C^3(\kappa - \alpha r)x \\ 0 & y_c(\gamma + 3\zeta x) & 2\lambda_C^2(\kappa - \alpha r)x \\ 2y_u\lambda_C^3 wx & 2y_c\lambda_C^2 wx & 1 + 3rx \end{pmatrix}, \tag{21}$$

where $w \equiv \eta - \gamma r + \alpha^*(\zeta - \gamma r)$. Equation (21) yields the following Higgs-to-charm coupling ratio in GMFV and in the SM:

$$c_c = \lambda(\gamma + 3\zeta x) \simeq 1 + 2\lambda\zeta x. \tag{22}$$

As $\lambda, \zeta \sim \mathcal{O}(1)$ and $x \lesssim 1$, $c_c > 1$ can be obtained for not too small values of x. As in all the above cases the coupling enhancement is at the cost of a moderate accidental cancellation among $\mathcal{O}(1)$ couplings. Note that the GMFV scale is constrained through the off-diagonal entries in Eq. (21) by a series of flavor changing observables analyzed in Ref. [16]. However, constraints from single-top production, neutral D meson mixing, flavor changing top decay $t \to hj$ and neutron electric dipole moment [assuming $\mathcal{O}(1)$ phases in the fundamental parameters] are satisfied for $x \lesssim 1$ since GMFV contributions are suppressed by λ_C^2, λ_C^5, λ_C^2 and $y_u\lambda_C^6$, respectively.

Consider finally composite pNGB Higgs models. Modifications of Higgs couplings to up-type quarks in composite Higgs models are parametrized by the effective Lagrangian in Eq. (15) with Λ replaced by the global symmetry breaking scale f, the "decay constant" of the pNGB Higgs [34]. The dimension-six coefficient in Eq. (15) receives two types of contributions from the composite dynamics, $g^u = g_h^u + g_\psi^u$. The first term is a direct contribution from the nonlinear Higgs dynamics and it is aligned with the marginal operator $g_h^u \propto \lambda^u$. The second term arises from the presence of light fermionic resonances from the strong dynamics. It is generically misaligned with λ^u and its entries scale like $g_\psi^u \sim \lambda^u \epsilon^2 (g_\psi f/m_\psi)^2$, where $g_\psi < 4\pi$ and m_ψ are, respectively, a typical strong coupling and a resonance mass of the strong dynamics, and $\epsilon < 1$ is the degree of the compositeness of the SM quarks. Neglecting flavor violation for simplicity and assuming relatively composite right-handed charm quark, the Higgs-to-charm coupling is [35]

$$c_c \simeq 1 + \mathcal{O}\left(\frac{v^2}{f^2}\right) + \mathcal{O}\left(\epsilon_c^2 \frac{g_\psi^2 v^2}{m_\psi^2}\right), \tag{23}$$

where ϵ_c is the right-handed charm degree of compositeness. The symmetry breaking scale f is constrained by EW precision parameters to be $f \gtrsim 750$ GeV (see e.g. [36,37] for a recent analysis). Hence, in the absence of light composite resonances associated with the charm quark, the Higgs-to-charm coupling is not expected to deviate significantly from its SM value. However, if light charm partner resonances are present a larger Higgs-to-charm can

be obtained. Current bounds on the charm partner mass from direct searches at the LHC are $m_\psi \gtrsim \mathcal{O}(500 \text{ GeV})$ [12]. Hence, for a fully composite charm quark $\epsilon_c \simeq 1$, $g_\psi \sim 4\pi$ a largely enhanced $hc\bar{c}$ coupling is possible.

V. CONCLUSIONS

We pointed out that the Higgs-to-charm coupling can be significantly enhanced, relative to its SM value, without conflicting with current Higgs data. As the dominant decay mode of the SM Higgs into bottom quarks is characterized by a rather small coupling, a moderate enhancement of the charm coupling is sufficient to yield dramatic changes in the Higgs phenomenology at the LHC. In particular, we find that current data even allow for the $h \to c\bar{c}$ mode to become the dominant Higgs decay channel. This results in the $h \to b\bar{b}$ signal strength being reduced down to $\mathcal{O}(40\%)$ level, which renders observation of this channel rather challenging for the next LHC run. However, we argued that a realistic prospective form of charm tagging would allow us to not only resurrect part of the lost $b\bar{b}$ signal but also to obtain signal strengths in the associated Higgs production channels which are close to the SM expectations by combining both charm and bottom pairs. We also briefly demonstrated that within several SM extensions an enhanced Higgs-to-charm coupling can be obtained through a moderate accidental cancellation between $\mathcal{O}(1)$ couplings of the theory.

ACKNOWLEDGMENTS

APPENDIX A: UNCONSTRAINED HIGGS FIT

We report for completeness the results of a global fit to all Higgs data in the most generic case where the eight free parameters c_V, $c_{c,b,t}$, c_τ, c_{gg}, $c_{\gamma\gamma}$ and $c_{Z\gamma}$ are allowed to deviate from their SM values. We use the freedom of redefining the Higgs boson phase to make $c_V > 0$, while the sign of the other parameters remains *a priori* unconstrained. However current Higgs data are insensitive to the sign of c_c and we assume $c_c > 0$ for simplicity. Following Ref. [3], we append the χ^2 function in Eq. (6) so as to include EW precision measurements from the LEP. The LEP measurements are dominantly sensitive to Higgs couplings to a weak gauge boson (c_V) and photons ($c_{\gamma\gamma}$ and $c_{Z\gamma}$), which modify the oblique EW parameters [38,39]. The global fit results are

$$c_V = 1.04^{+0.04}_{-0.04}, \qquad c_t = 0.9^{+1.0}_{-2.7}, \qquad c_c = 2.9^{+2.9}_{-2.9},$$
$$c_b = 1.26^{+0.33}_{-0.31}, \qquad c_\tau = 1.19^{+0.25}_{-0.27}, \qquad c_{gg} = 0.004^{+0.035}_{-0.043},$$
$$c_{\gamma\gamma} = 0.0005^{+0.0026}_{-0.0063}, \qquad c_{Z\gamma} = -0.003^{+0.022}_{-0.036}. \qquad \text{(A1)}$$

Note that the combination $c_{gg} + 1.26 \times 10^{-2} c_t$, which approximately controls the gluon fusion cross section, is unconstrained by signal strength measurements. In general, when deriving the standard deviations in Eq. (A1), we discarded isolated minima away from the SM where large values of c_{gg} cancel against a significantly modified SM top loop contribution in $\sigma_{gg \to h}$ to yield small deviations in Higgs rates.

APPENDIX B: HIGGS COUPLINGS IN GMFV

In GMFV models the Lagrangian relevant to Higgs couplings of the up-type quark sector read [29]

$$\mathcal{L}_{\text{GMFV}} = \mathcal{L}_1 + \mathcal{L}_3, \qquad \text{(B1)}$$

with the marginal operators

$$\mathcal{L}_1 = \lambda(\bar{Q}_3 \tilde{H} U_3 + \alpha \bar{Q}_a \tilde{H} \chi^a U_3 \\ + \beta \bar{Q}_3 \tilde{H} \chi^a \phi_u^{ab} U_b + \gamma \bar{Q}_a \tilde{H} \phi_u^{ab} U_b) + \text{H.c.}, \qquad \text{(B2)}$$

and the dimension-six operators

$$\mathcal{L}_3 = \frac{g}{\Lambda^2} H^\dagger H (\bar{Q}_3 \tilde{H} U_3 + \kappa \bar{Q}_a \tilde{H} \chi^a U_3 \\ + \eta \bar{Q}_3 \tilde{H} \chi^a \phi_u^{ab} U_b + \zeta \bar{Q}_a \tilde{H} \phi_u^{ab} U_b) + \text{H.c.}, \qquad \text{(B3)}$$

where $\alpha, \beta, \gamma, \kappa, \eta$ and ζ are complex $\mathcal{O}(1)$ numbers. $a, b = 1, 2$ are the first two generation indices, while index $_3$ denotes the third generation. In the mass basis the spurions become $\phi_u \propto (m_u, m_c)$ and $\chi \sim (V_{ts}, V_{td}) \sim (\lambda_C^3, \lambda_C^2)$, where V_{ij} are CKM matrix elements and $\lambda_C \simeq 0.23$ is the sine of the Cabibbo angle. Higher-order terms in ϕ_u and χ are neglected. A similar Lagrangian can be written for the down-type quark sector. The Lagrangian of Eq. (B1) yields the following mass matrix

$$M^u = \frac{\lambda v}{\sqrt{2}} \begin{pmatrix} y_u(\gamma + x\zeta) & 0 & \chi_1(\alpha + \kappa x) \\ 0 & y_c(\gamma + \zeta x) & \chi_2(\alpha + \kappa x) \\ y_u \chi_1(\gamma + \eta x) & y_c \chi_2(\gamma + \eta x) & 1 + rx \end{pmatrix}, \qquad \text{(B4)}$$

and Higgs coupling matrix

$$Y^u = \frac{\lambda}{\sqrt{2}} \begin{pmatrix} y_u(\gamma + 3\zeta x) & 0 & \chi_1(\alpha + 3\kappa x) \\ 0 & y_c(\gamma + 3\zeta x) & \chi_2(\alpha + 3\kappa x) \\ y_u \chi_1(\gamma + 3\eta x) & y_c \chi_2(\gamma + 3\eta x) & 1 + 3rx \end{pmatrix}, \qquad \text{(B5)}$$

where we defined $x \equiv v^2/(2\Lambda^2)$.

[1] G. Aad *et al.* (ATLAS Collaboration), Phys. Lett. B **716**, 1 (2012).

[2] S. Chatrchyan *et al.* (CMS Collaboration), Phys. Lett. B **716**, 30 (2012).

[3] A. Falkowski, F. Riva, and A. Urbano, J. High Energy Phys. 11 (**2013**) 111.

[4] P. P. Giardino, K. Kannike, I. Masina, M. Raidal, and A. Strumia, arXiv:1303.3570.

[5] Z.-z. Xing, H. Zhang, and S. Zhou, Phys. Rev. D **77**, 113016 (2008);Z.-z. Xing, H. Zhang, and S. Zhou, Phys. Rev. D **86**, 013013 (2012).

[6] G. Aad *et al.* (ATLAS Collaboration), Report No. ATLAS-CONF-2013-068, 2013.

[7] G. T. Bodwin, F. Petriello, S. Stoynev, and M. Velasco, Phys. Rev. D **88**, 053003 (2013).

[8] S. Chatrchyan *et al.* (CMS Collaboration), arXiv:1310.1138.

[9] R. Mahbubani, M. Papucci, G. Perez, J. T. Ruderman, and A. Weiler, Phys. Rev. Lett. **110**, 151804 (2013).

[10] M. Blanke, G. F. Giudice, P. Paradisi, G. Perez, and J. Zupan, J. High Energy Phys. 06 (**2013**) 022.

[11] L. Da Rold, C. Delaunay, C. Grojean, and G. Perez, J. High Energy Phys. 02 (**2013**) 149.

[12] C. Delaunay, T. Flacke, J. Gonzalez-Fraile, S. J. Lee, G. Panico, and G. Perez, arXiv:1311.2072.

[13] S. Fajfer, A. Greljo, J. F. Kamenik, and I. Mustac, J. High Energy Phys. 07 (**2013**) 155.

[14] N. D. Christensen, T. Han, and Y. Li, Phys. Lett. B **693**, 28 (2010);N. Desai, D. K. Ghosh, and B. Mukhopadhyaya, Phys. Rev. D **83**, 113004 (2011);C. Englert, D. Goncalves-Netto, K. Mawatari, and T. Plehn, J. High Energy Phys. 01 (**2013**) 148;R. Godbole, D. J. Miller, K. Mohan, and C. D. White, arXiv:1306.2573.

[15] C. Delaunay, G. Perez, H. de Sandes, and W. Skiba, arXiv:1308.4930.

[16] R. Harnik, J. Kopp, and J. Zupan, J. High Energy Phys. 03 (**2013**) 026.

[17] D. Carmi, A. Falkowski, E. Kuflik, T. Volansky, and J. Zupan, J. High Energy Phys. 10 (**2012**) 196.

[18] G. Belanger, B. Dumont, U. Ellwanger, J. F. Gunion, and S. Kraml, Phys. Rev. D **88**, 075008 (2013).

[19] G. Aad *et al.* (ATLAS Collaboration), Phys. Lett. B **726**, 88 (2013).

[20] S. Chatrchyan *et al.* (CMS Collaboration), Report No. CMS-PAS-HIG-12-042, 2012;S. Chatrchyan *et al.* (CMS Collaboration), Report No. CMS-PAS-HIG-12-044, 2012;S. Chatrchyan *et al.* (CMS Collaboration), Report No. CMS-PAS-HIG-13-001, 2013;S. Chatrchyan *et al.* (CMS Collaboration), Report No. CMS-PAS-HIG-13-002, 2013;S. Chatrchyan *et al.* (CMS Collaboration), Report No. CMS-PAS-HIG-13-004, 2013;S. Chatrchyan *et al.* (CMS Collaboration), Report No. CMS-PAS-HIG-13-009, 2013.

[21] T. Aaltonen *et al.* (CDF and D0 Collaborations), Phys. Rev. D **88**, 052014 (2013).

[22] S. Chatrchyan *et al.* (CMS Collaboration), Report No. CMS-PAS-HIG-13-003, 2013.

[23] S. Chatrchyan *et al.* (CMS Collaboration), arXiv:1310.3687 [Phys. Rev. D (to be published)].

[24] S. Chatrchyan *et al.* (CMS Collaboration), Report No. CMS-PAS-HIG-13-011, 2013.

[25] S. Chatrchyan *et al.* (CMS Collaboration), Phys. Lett. B **726**, 587 (2013).

[26] J. Baglio *et al.* (LHC Higgs Cross Section Working Group), CERN Report No. CERN-2011-002, 2011;S. Alekhin *et al.* (LHC Higgs Cross Section Working Group), CERN Report No. CERN-2012-002, 2012.

[27] A. D. Martin, W. J. Stirling, R. S. Thorne, and G. Watt, Eur. Phys. J. C **63**, 189 (2009).

[28] R. V. Harlander and W. B. Kilgore, Phys. Rev. D **68**, 013001 (2003).

[29] A. L. Kagan, G. Perez, T. Volansky, and J. Zupan, Phys. Rev. D **80**, 076002 (2009).

[30] M. Trott and M. B. Wise, J. High Energy Phys. 11 (**2010**) 157.

[31] M. Jung, A. Pich, and P. Tuzon, J. High Energy Phys. 11 (**2010**) 003.

[32] A. Dery, A. Efrati, G. Hiller, Y. Hochberg, and Y. Nir, J. High Energy Phys. 08 (**2013**) 006.

[33] J. F. Gunion and H. E. Haber, Phys. Rev. D **67**, 075019 (2003).

[34] G. F. Giudice, C. Grojean, A. Pomarol, and R. Rattazzi, J. High Energy Phys. 06 (**2007**) 045.

[35] C. Delaunay, C. Grojean, and G. Perez, J. High Energy Phys. 09 (**2013**) 090.

[36] C. Grojean, O. Matsedonskyi, and G. Panico, J. High Energy Phys. 10 (**2013**) 160.

[37] M. Ciuchini, E. Franco, S. Mishima, and L. Silvestrini, J. High Energy Phys. 08 (**2013**) 106.

[38] M. E. Peskin and T. Takeuchi, Phys. Rev. Lett. **65**, 964 (1990).

[39] R. Barbieri, A. Pomarol, R. Rattazzi, and A. Strumia, Nucl. Phys. **B703**, 127 (2004).